

Raman Spectroscopy and Raman Imaging in the Characterization of Radiation-Induced Biomarkers in MDA-MB-231 Breast Cancer Cells

Seok-Jin Kim ^a, Rodrigo Hernández Millares ^a, Kiok Han ^a, Sung-Joon Ye ^{a, b, c, d*}

^aDepartment of Applied Bioengineering, Graduate School of Convergence Science and Technology, Seoul National University, 08826, Seoul, Republic of Korea

^bResearch Institute of Convergence Science, Seoul National University, 08826, Seoul, Republic of Korea

^cAdvanced Institute of Convergence Technology, Seoul National University, 16229, Suwon, Republic of Korea

^dBiomedical Research Institute, Seoul National University Hospital, 03080, Seoul, Republic of Korea

*Corresponding author: sye@snu.ac.kr

1. Introduction

Raman spectroscopy has attracted significant interest within the scientific community as a non-invasive method due to its capacity for precise identification of biomolecules and its sensitivity in accurately conveying diagnostic insights regarding molecular signature alterations within cells or tissues. Furthermore, Raman imaging has demonstrated promise as a viable approach for visualizing intracellular dynamics. [1-2]

Raman spectroscopy offers substantial advantages not only in cancer diagnostics but also in elucidating the cellular response to cancer treatments such as radiation therapy. Its potential lies in uncovering the mechanisms underlying the radiosensitivity of cancer cells, with the goal of enhancing the precision of treatment responses. [3-4]

In this investigation, Raman spectroscopic analytical techniques were employed in conjunction with Raman imaging to delineate the biomolecular profiles implicated in the cellular reaction to external X-ray irradiation. Cellular imaging was conducted utilizing Raman peaks associated with the radiation response, in conjunction with the Raman spectrum derived from specific organelles of interest (Nucleus and cytoplasm).

2. Materials and Methods

2.1 Cell Culture

Breast cancer cells MDA-MB-231 were purchased from the Cell Line Bank (Seoul, Korea) and cultured in RPMI 1,640 containing 1% penicillin/streptomycin and 10% fetal bovine serum. Cells were cultured on a calcium fluoride (CaF₂) substrate within a petri dish containing phosphate-buffered saline (PBS). Before and after X-ray treatment, the cells were maintained in an incubator. Subsequently, the cells were fixed with a fixation solution (4% paraformaldehyde for 30 min) prior to Raman analysis.

2.1 Cell Irradiation

The X-RAD 320 system, Precision X-ray Inc., North Branford, CT, was utilized for irradiation purposes. The irradiation procedure followed the in-air method as outlined in the AAPM TG-61 protocol for radiotherapy

and radiobiology. An X-ray beam energy of 300 kVp was employed, with a field size of 10 × 10 cm and a source-to-surface distance (SSD) of 50 cm. The cell samples were subjected to either an irradiation dose of 8 Gy or remained non-irradiated (0 Gy). Following irradiation, the cells were incubated for 24 hours in an incubator before being fixed.

2.1 Raman experimentation and analysis

Raman spectroscopy acquisition utilized a 532 nm laser, employing a 60 x water immersion objective. The laser power applied on the sample was set to 20 mW. Prior examination of cells under brightfield microscopy informed the selection of a region of interest (ROI) measuring 30 μm by 30 μm, with a step size of 0.5 μm, encompassing both cellular and extracellular regions.

The obtained Raman spectra underwent preprocessing steps, including background correction, smoothing, and removal of cosmic ray artifacts. Subsequently, an in-house MATLAB algorithm was devised to visualize the maximum intensity of Raman peaks of interest. Principal component analysis (PCA) was employed to discern the primary distinctions between the unirradiated and irradiated cells.

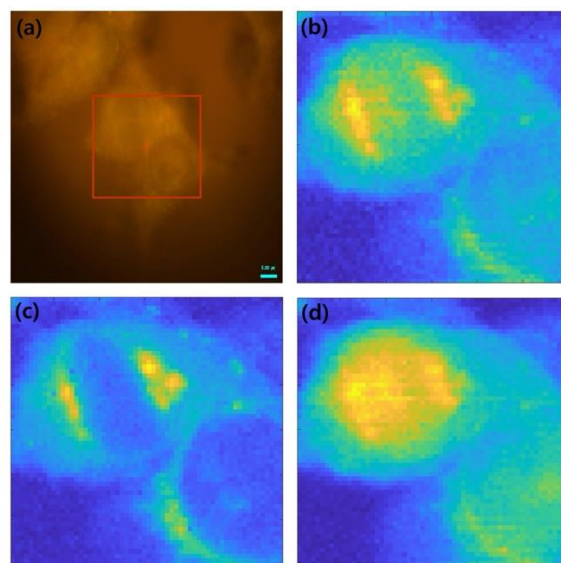


Fig. 1. a) Microscope image of MDA-MB-231 cells, the red box corresponds to the ROI. Raman images of the peaks corresponding to b) 1469 cm⁻¹, c) 2900 cm⁻¹ and d) 3012 cm⁻¹

3. Results and Discussion

3.1 Raman Imaging

Fig. 1 a illustrates the brightfield image of a single MDA-MB-231 cancer cell. The corresponding Raman images from different peaks is shown in Fig. 1 b, c, and d. The Raman images closely align with the microscope image, indicating a correlation between structural and biochemical features. Each Raman image portrays distinct biochemical characteristics of the sample, thereby supplementing optical information with valuable insights into its bio composition.

3.1 Raman Analysis

The Raman spectra derived from the nucleus and cytoplasm were extracted from the previously acquired images. Subsequently, the average spectrum was computed and normalized to yield the characteristic Raman spectrum for each organelle from both irradiated and unirradiated cells. Figure 2 a and b display the representative Raman spectrum obtained from the nucleus and cytoplasm in both irradiated and non-irradiated samples. The figure demonstrates distinct variations in peak wavenumbers and intensities within the Raman spectrum, depending on the experimental location.

Moreover, PCA was conducted to identify the peaks exhibiting significant variation between cells irradiated with 8 Gy and non-irradiated cells. The PCA analysis revealed Raman peaks that experienced shifts in wavenumber or modifications in intensity due to radiation treatment. These identified peaks have the potential to serve as Raman biomarkers indicative of radiation response.

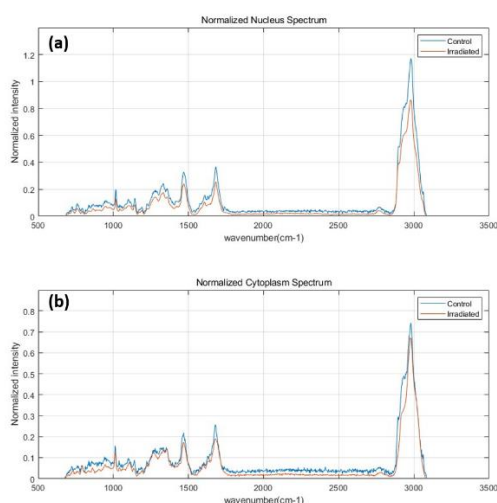


Fig. 2. Representative Raman spectra extracted from cellular components, comparing irradiated and non-irradiated samples. a) Spectrum derived from the nucleus, and b) spectrum derived from the cytoplasm.

4. Conclusions

In conclusion, this study successfully generated Raman images of cells irradiated with X-rays and identified key Raman peaks that may function as biomarkers. These biomarkers hold promise for further analysis and correlation with the response to radiation treatment, thereby facilitating the assessment of cellular radiosensitivity.

Acknowledgements

This work was supported by a National Research Foundation of Korea (NRF) grant funded by the Korea government (MSIT) (No. RS-2023-00237149).

REFERENCES

- [1] S. Elumalai, S. Managó, and A.C. De Luca, Raman microscopy: progress in research on cancer cell sensing, *Sensors*, Vol. 20, p. 5525, 2020.
- [2] J. Xu, T. Yu, C.E. Zois, J-X. Cheng, Y. Tang, A.L. Harris, and W.E. Huang, Unveiling cancer metabolism through spontaneous and coherent Raman spectroscopy and stable isotope probing, *Cancers*, Vol. 13, p. 1718, 2021.
- [3] S.J. Van Nest, L.M. Nicholson, N. Pavey, M. N. Hindi, A. G. Brolo, A. Jirasek, and J. J. Lum, Raman spectroscopy detects metabolic signatures of radiation response and hypoxic fluctuations in non-small cell lung cancer, *BMC Cancer*, Vol. 19, p. 474, 2019.
- [4] M. Kopec, M. Blaszczyk, M. Radek, and H. Abramczyk, Raman imaging and statistical methods for analysis various type of human brain tumors and breast cancers, *Spectrochim. Acta - A: Mol. Biomol. Spectrosc.*, Vol. 262, p. 120091, 2021.